



## OPEN ACCESS

EDITED BY  
Chong Xu,  
Ministry of Emergency Management,  
China

REVIEWED BY  
Kaizong Xia,  
Institute of Rock and Soil Mechanics  
(CAS), China  
Danqing Song,  
Tsinghua University, China

\*CORRESPONDENCE  
Xiaoyong Lian,  
bqt2000101013@student.cumtb.edu.cn

SPECIALTY SECTION  
This article was submitted to  
Geohazards and Georisks,  
a section of the journal  
Frontiers in Earth Science

RECEIVED 09 August 2022  
ACCEPTED 13 September 2022  
PUBLISHED 10 January 2023

CITATION  
Lian X, Li C, Li J and Wu L (2023), Law of  
strata pressure behavior of surrounding  
rock in nearby goaf roadway for extra-  
thick coal seams of Datong mine area.  
*Front. Earth Sci.* 10:1015378.  
doi: 10.3389/feart.2022.1015378

COPYRIGHT  
© 2023 Lian, Li, Li and Wu. This is an  
open-access article distributed under  
the terms of the [Creative Commons  
Attribution License \(CC BY\)](https://creativecommons.org/licenses/by/4.0/). The use,  
distribution or reproduction in other  
forums is permitted, provided the  
original author(s) and the copyright  
owner(s) are credited and that the  
original publication in this journal is  
cited, in accordance with accepted  
academic practice. No use, distribution  
or reproduction is permitted which does  
not comply with these terms.

# Law of strata pressure behavior of surrounding rock in nearby goaf roadway for extra-thick coal seams of Datong mine area

Xiaoyong Lian<sup>1,2\*</sup>, Chen Li<sup>3</sup>, Jun Li<sup>1</sup> and Liang Wu<sup>2</sup>

<sup>1</sup>China University of Mining and Technology (Beijing), Beijing, China, <sup>2</sup>Uroica (Shandong) Mining Technology Co., Ltd., Taian, China, <sup>3</sup>CCTEG Wuhan Engineering Company, Wuhan, China

The nearby goaf road in the extra-thick coal seam of the Datong mining area exhibits intense strata pressure behavior, which affects the working face mining. Herein, we study the laws of the strata pressure behavior of this road in detail using various methods, including laboratory tests, theoretical analyses, numerical simulation, and field monitoring. Considering the mine pressure characteristics of the nearby goaf road, namely, roof cracking, two-side deformation, and floor heaving, the mechanical tests and theoretical failure analyses of the surrounding rock in the mining-induced non-uniform stress field were carried out. The circular-oval-butterfly failure trend of the surrounding rock in the nearby goaf road under the influence of mining was obtained. The steady failure evolution lateral pressure coefficient ( $\lambda=0.5\sim 1.8$ ) and butterfly mutation lateral pressure coefficient ( $\lambda<0.35$  or  $\lambda>2.1$ ) of the surrounding rock in the nearby goaf road were analyzed. We performed numerical simulation to study the stress field and the plastic zone shape-size characteristics of the surrounding rock during excavation and mining (with or without the top extraction road), and the theoretical law of the mine pressure was obtained for the Tong Xin coal mine. Finally, field monitoring indicates that the mine pressure behavior of the nearby goaf road exhibits spatial differences, namely, the difference between the stresses of the two sides and roof, and the stress characteristics of the deep and shallow surrounding rock. The findings of this study on the mine pressure behavior in the nearby goaf road have great practical significance for targeted measures to control the surrounding rock stability.

## KEYWORDS

nearby goaf roadway, butterfly plastic zone, numerical simulation, top excavating roadway, lateral pressure coefficient

## Introduction

Most of China's coal resources rely on underground mining. The stability control of the surrounding rock in the road is key to the underground coal mining and the premise of coal mine safety, high efficiency, and production (Hongpu et al., 2019; Hongpu 2020). To ensure the stability of the surrounding rock of the mining-affected road, most mines in China adopt the method of retaining large coal pillars to protect the road. However, the road will still be subject to continuous deformation and failure under the action of the high deviant stress field caused by the nearby goaf (Detournay and John 1988; Ding et al., 2021; Zhang et al., 2021).

In contrast to the remaining road along the goaf of the dual-carriageway arrangement, the road layout along the goaf can reduce the times of road travel affected by the dynamic pressure. However, the high deviational stress environment of the nearby goaf causes the severe mining pressure manifestation of the road while driving (Li et al., 2020a; Li et al., 2020b). Scholars at home and abroad have carried out many targeted studies on the mechanism of the mine pressure development in mining-affected roads (Li et al., 2022; Qihang et al., 2022).

Considering mining stress, based on the stress environment analysis of goaf driving, Wang et al. (Xie et al., 2016; Xie et al., 2019) analyzed the abutment pressure distribution characteristics of the integrated coal beside the road using damage theory, as well as the qualitative relationship between the abutment pressure and several other parameters such as the thickness of the direct roof and elastic modulus. These results have great significance for guiding the maintenance of the goaf road. Xie et al. (Xie et al., 2016; Xie et al., 2019; Qingfeng et al., 2020) obtained the theoretical position formula and distribution characteristics of the peak stress of the coal pillar by analyzing many fields measuring the data of abutment pressure of the coal pillar in the fully mechanized mining face of a medium-thick coal seam, and employing the relevant theories of elastic mechanics and elastic-plastic mechanics. The column width effect of the overburden stress and caving height, the mechanical characteristics of the stress shell of the surrounding rock in the road, and the evolution characteristics of the surrounding rock force chain at the working face were likewise obtained. In terms of deformation and failure, Bai et al. (Jian-biao et al., 2007; Chaojiong et al., 2021) used FLAC numerical simulation software to calculate the relationship between deformation and time in the surrounding rock, and determined the reasonable secondary support time according to the characteristics of the concentrated stress around the road and the overall severe deformation. Chen et al. (Deng-hong et al., 2016; Pu et al., 2020; Tian and Yiliang 2020) simulated and analyzed the strain characteristics of the surrounding rock under gradient action. The different strain state characteristics of the shallow-deep surrounding rock in the road were obtained under the condition of shallow buried depth and homogeneous pressure.

Meanwhile, the strain distribution characteristics of the alternating tension-pressure were studied in a radial direction road under the state of deep buried homogeneous pressure. In terms of the damage mechanism of the surrounding rock, Zhao (Zhiqiang 2014; Zhao et al., 2018) derived the plastic zone boundary equation of the surrounding rock in the circular road under the non-uniform stress field, explained the non-uniform large deformation on the road, and provided the basis for the theory of the "butterfly plastic zone." Jia et al. (Housheng et al., 2016; Jia et al., 2019) studied the interlayer penetration of the butterfly plastic zone and claimed that the high-strength rock strata could not prevent the formation and expansion of butterfly blades in the deep weak rock strata. Guo et al. (Guo et al., 2019; Xiaofei 2019; Guo et al., 2020) studied the shape of the plastic zone under different confining pressures based on the boundary invisibility equation of the butterfly plastic zone and obtained the criterion for determining its shape. Liu et al. (Hongtao et al., 2017; Chen et al., 2019) took the Shigetai coal mine as their research background, and performed numerical analysis on the plastic zone distribution characteristics of retaining the road with the dual-carriageway arrangement. They studied the vector deflection of the principal stress and explained the mechanism of the deformation inhomogeneity of the remaining road based on plastic zone deflection.

However, with the geological condition of the hugely thick coal seam in the Datong mining area, research studies on the non-isobaric failure mechanism of the mining road are relatively few. Based on the actual situation of severe deformation and the failure of the mining road in the Datong mining area, the corresponding relationship between the surrounding rock stress and the plastic zone of the non-isobaric nearby goaf road was studied in theoretical analysis of the stress relationship in the mining road. The evolution law of the surrounding rock pressure in the nearby goaf road was studied based on field observation of the mine pressure, which has a reference value for the stability control of the rock surrounding the road in this mining area.

## Engineering background

### Engineering and geological profiles

Due to the special coal forming environment of the carboniferous coal seam in the Datong coalfield, the stability of the surrounding rock is poor, and there is a risk of its instability. The geological conditions of the Tong Xin coal mine are in line with the evolution characteristics of the Datong coalfield. Taking the Tong Xin coal mine as the research background, the characteristics of the extra-thick coal seam in the Datong coalfield can be studied. The Tong Xin coal mine is currently mainly mining a 8# coal seam. The average thickness of the coal seam is 21.5 m. The average buried depth is 447 m. The top coal caving mining method was adopted this time. The road arrangement is to drive near the goaf. To avoid the gas

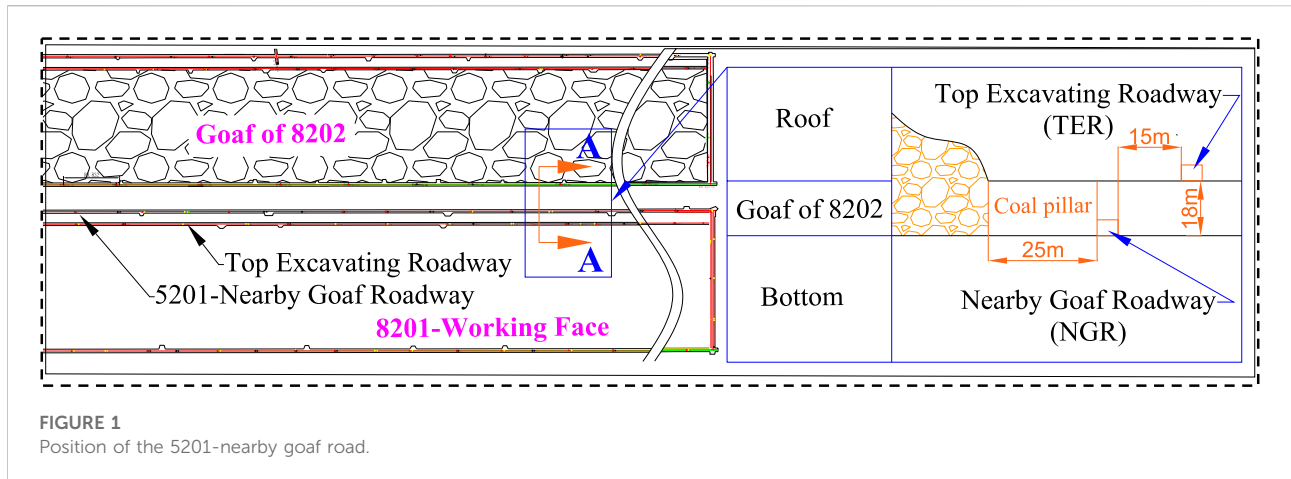


FIGURE 1  
Position of the 5201-nearby goaf road.



FIGURE 2  
Failure state of the surrounding rock in the nearby goaf road.

overlimit, a top extraction road was pre-excavated at the top of the coal seam to pre-drain the gas. The locations of the relevant road and goaf are shown in Figure 1. The stress state of the surrounding rock in the 5201-road changes significantly under the dual influence of the top extraction road and the nearby 8202 goaf.

## Deformation and failure of the nearby goaf road

The spatial position relationship between the lateral goaf and the nearby goaf road indicates that the road must be driven on within the influence range of the mining-induced abutment

pressure. Therefore, there is a significant manifestation of mine pressure during the excavating period, and the roof grouting will break after some time, as shown in Figure 2A. When the 8201 working face is mined, the nearby goaf road is further affected by the advanced mining, and the surrounding rock is in a state of bidirectional stress superposition. The rapid change of stress leads to the further aggravation of the road deformation, such as the road side bulge (Figure 2B), floor heave (Figure 2C), and support failure (Figure 2D).

Therefore, the stability of the surrounding rock in the nearby goaf road has great hidden danger. The process of the mining stress causing damage to the nearby goaf road must be studied systematically. Moreover, methods for maintaining stability in

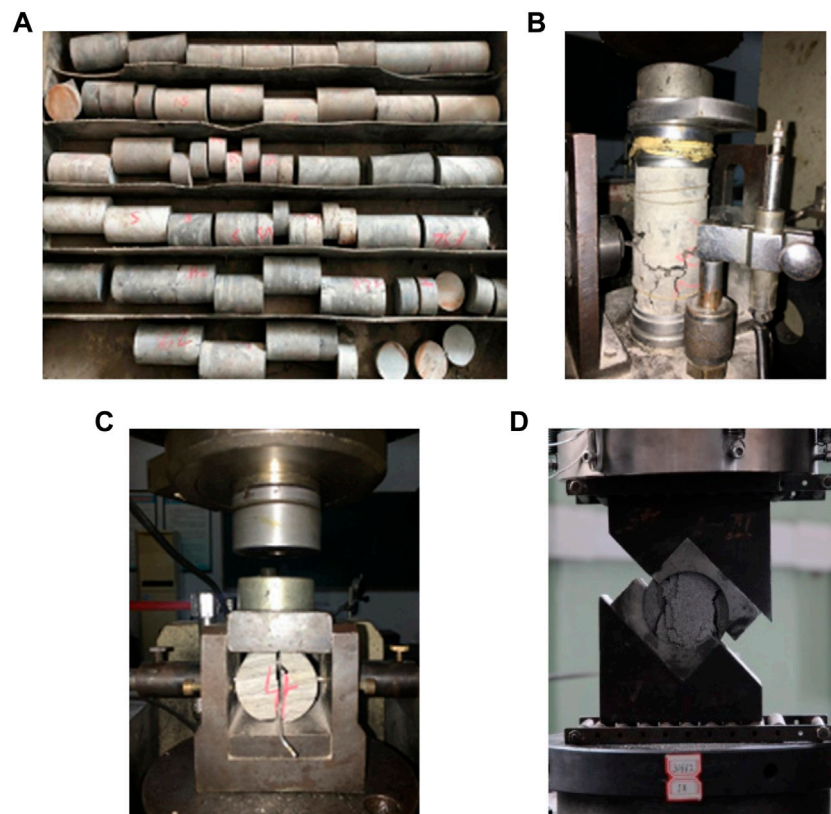


**FIGURE 3**  
Test process of rock mechanics.

the nearby goaf road and the corresponding control measures of the surrounding rock must be addressed in detail.

## Mechanical parameters test of the surrounding rock

When the external stress on the surrounding rock is greater than its ultimate strength, the rock undergoes plastic failure, which is the fundamental failure reason of the surrounding rock in roads (Zhen 2018; Guo et al., 2021). To master the characteristics of the carboniferous strata and study the failure mechanism of the surrounding rock of the nearby goaf road, the rock core was drilled out on the roof and floor of the 3~5# coal seam in the 8201-working face of the Tong Xin coal mine. The rock core size spans 75 mm in diameter and 20 m in depth, as shown in Figure 3A. The mechanical parameters of the surrounding rock samples were measured in accordance with “GB/T 23561-2009 Method for the Determination of Physical and Mechanical Properties of Coal and Rock.” The uniaxial compressive strength test, tensile strength test, and variable shear test were carried out in rock mechanics experiments

(Du et al., 2020; Du and Song 2022). The rock specimens and test process are illustrated in Figure 3. The approximate mechanical parameters of the surrounding rock were obtained by the laboratory rock mechanics test using the Hoek–Brown strength criterion (Kaizong et al., 2022; Xia et al., 2022). The final rock parameters in Table 1 are adjusted based on the investigation of the rock structure characteristics and the analysis of the rock disturbance.

## Stability analysis of the surrounding rock of the nearby goaf road

### Theoretical calculation

After the working face mining, the surrounding rock of the nearby goaf road is in a non-uniform stress state due to the lateral horizontal stress unloading and the vertical stress concentration. Therefore, the traditional failure theory of the surrounding rock under constant pressure is no longer applicable to the mining-affected road. The surrounding rock environment of the dynamic pressure circular road is regarded as isotropic ideal elastic-plastic



TABLE 1 Mechanical parameters of the surrounding rock of the nearby goaf road.

Lithology	Density/kg/ m <sup>3</sup>	Bulk modulus/ MPa	Shear modulus/MPa	Cohesion/ MPa	Internal friction angle/ <sup>o</sup>	Tensile strength/MPa
Medium coarse-grained sandstone	2,660	2,600	2,910	2.4	30	0.5
Coal	1,350	1,300	2000	1	20	0.3
Pebbled coarse sandstone	2,660	2,250	2,450	3	31	1.2
Carbon mudstone	2,560	4,730	3,700	1.3	27	0.3
Kaolinite mudstone	2,551	5,640	5,950	1.3	27	0.76
Packsand	2,670	6,630	7,230	8.7	37	2.1
Siltstone	2,170	2,790	3,050	2.1	29	0.5

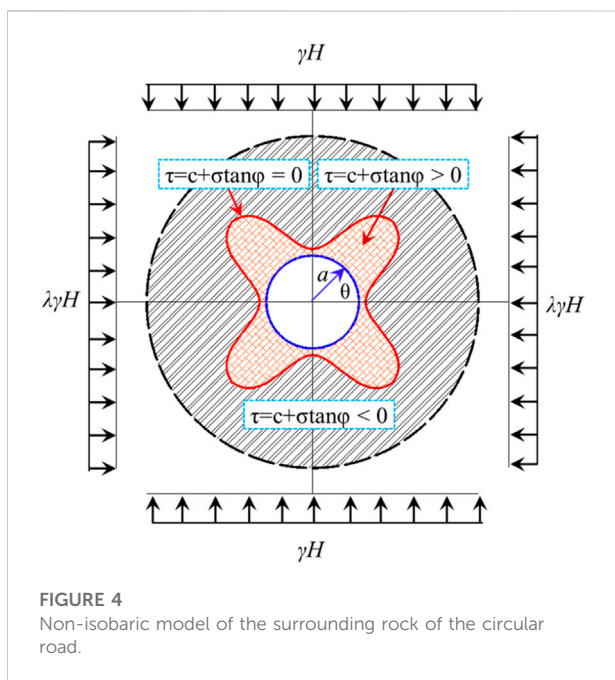


FIGURE 4 Non-isobaric model of the surrounding rock of the circular road.

material. The nearby goaf road is treated as a problem of an infinite plane strain (Yongen et al., 2021). The Mohr–Coulomb strength criterion is employed for analysis, and the theoretical model is shown in Figure 4.

The boundary equation of the plastic zone in the surrounding rock of the non-isobaric circular road can be expressed as:

$$(1 - \lambda)^2 - \sin^2 \varphi \left( 1 + \lambda + \frac{4C \cos \varphi}{\gamma H \sin \varphi} \right)^2 + \left[ 2(1 - \lambda^2) \cos 2\theta \cos 2\varphi - 4(1 - \lambda)^2 \cos 4\theta - \frac{4C}{\gamma H} (1 - \lambda) \sin 2\varphi \cos 2\theta \right] \left( \frac{a}{r} \right)^2 + \left[ (1 + \lambda)^2 - 2(1 - \lambda)^2 (1 + 2 \cos 2\theta) + 4(1 - \lambda)^2 (2 + \cos^2 \varphi) \cos^2 2\theta \right] \left( \frac{a}{r} \right)^4 + \left[ 6(1 - \lambda^2) \cos 2\theta - 12(1 - \lambda)^2 \right] \left( \frac{a}{r} \right)^6 + \left[ 9(1 - \lambda)^2 \right] \left( \frac{a}{r} \right)^8 = 0$$

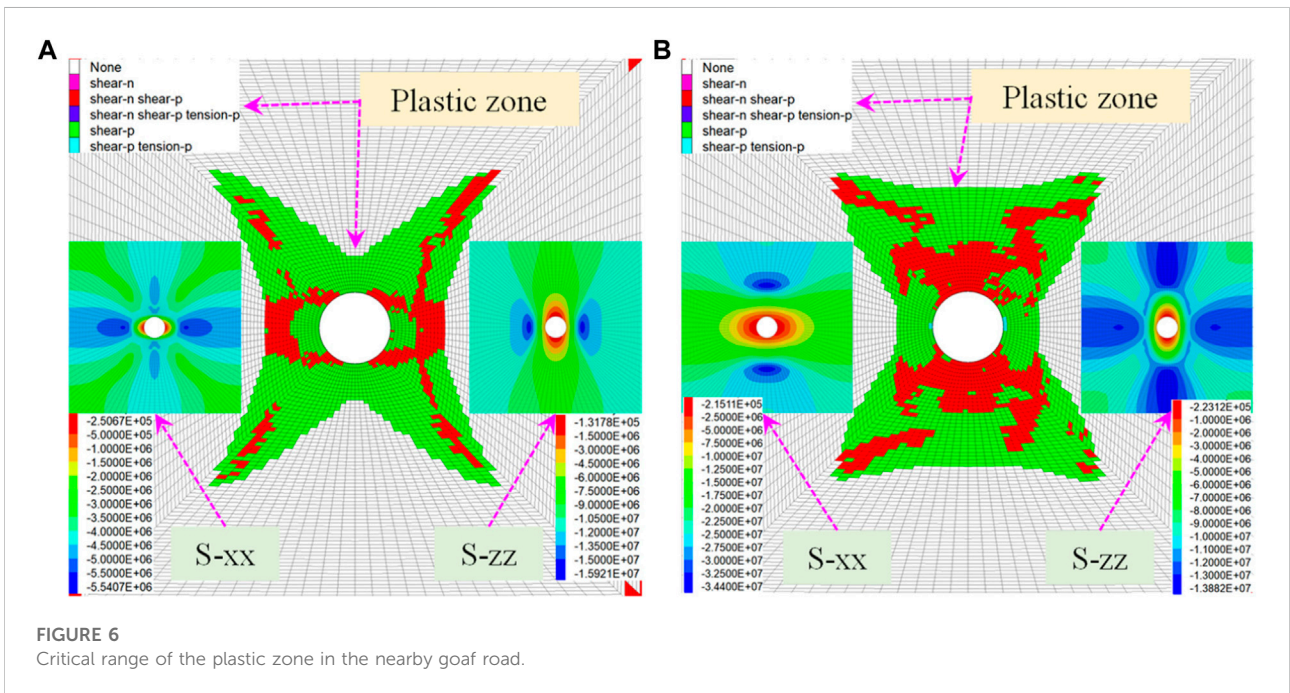
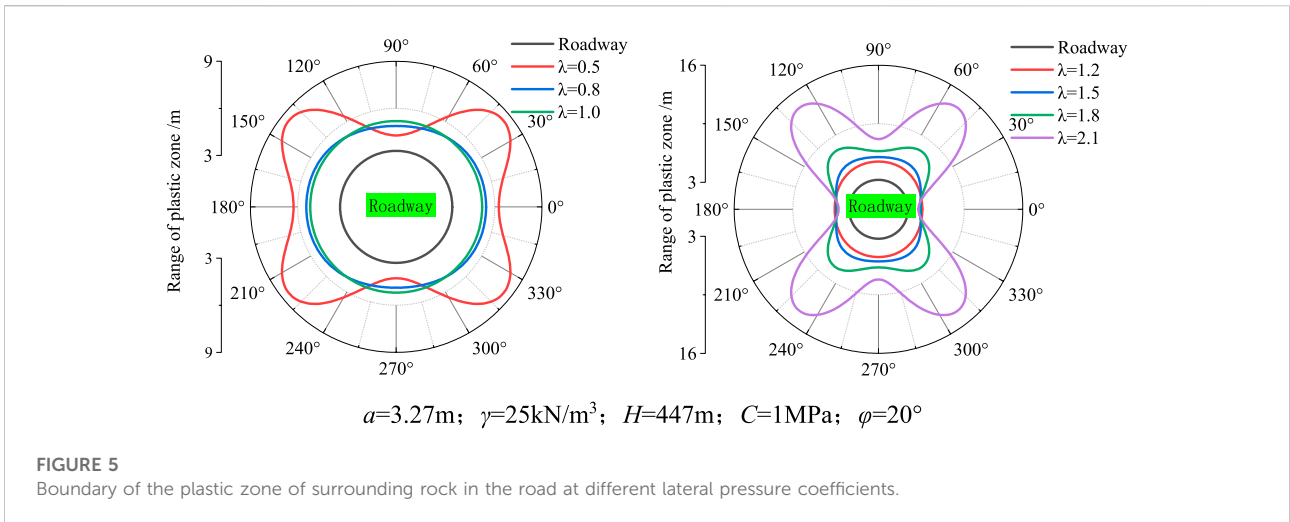
Herein,  $\lambda$  is the lateral pressure coefficient;  $a$  is the roadway radius;  $\gamma$  is the unit weight of rock stratum;  $H$  is the buried depth of the roadway; and  $C$  and  $\varphi$  are the cohesion and internal friction angle of the coal rock medium, respectively.

There are numerous limiting conditions for theoretical analysis of the stress distribution, and there is currently no clear theoretical formula for the complex road sections. Therefore, the theoretical analysis of a circular road section can be used as a reference. The 5201-nearby goaf road is a rectangular section with a net area of 19.24 m<sup>2</sup>, and its equivalent circle radius is 3.27 m. The physical and mechanical parameters of the 3–5# coal seam are taken as the basis for the theoretical calculation, and calculated repeatedly using the C# program. The calculated results are shown in Figure 5.

The lateral pressure coefficients have a large impact on the surrounding rock plastic area of road. At different lateral pressure coefficients, the plastic zone of the surrounding rock in the road has three shapes, namely, circular, oval, and butterfly. When the plastic zone of the road is butterfly-shaped, it increases rapidly, making the road most difficult to maintain in this situation. Moreover, when the conditions of the road’s buried depth and the mechanical parameters of the rock are fixed, the shape of the plastic zone in the road is only related to the lateral pressure coefficient  $\lambda$ . Therefore, the shape of the plastic zone can be taken as the condition of road stability, as a change in the lateral pressure coefficient of the nearby goaf road is an important prerequisite for the butterfly instability of the surrounding rock in the road.

To elucidate the influence of the different lateral pressure coefficient on the plastic zone of the surrounding rock in the nearby goaf road, the FLAC3D numerical analysis method is used for analysis [30, 31]. Under the specific geological conditions of the Tong Xin coal seam, the lateral pressure coefficient is very small (<0.35) or great (>2.1), all leading to the butterfly deterioration of the plastic zone, which is not conducive to the maintenance of road stability, as shown in Figure 6. If the surrounding rock stress under a limited state increases further, the complete instability of the surrounding rock will take place in the plastic zone of the road.

However, the shape and size of the plastic zone of the surrounding rock in the nearby goaf road of Tong Xin coal mine gradually and steadily evolves within a certain range. As



shown in Figure 7, the lateral pressure coefficient increases from 0.5 to 1.0, achieving a lateral pressure coefficient change rate of 100%, and the shape of the plastic zone gradually grows from the horizontal ellipse to the circle. When  $\lambda = 1.0$ , the plastic zone shape is circular. When the lateral pressure coefficient ranges from 1.0 to 1.8, the lateral pressure coefficient variation rate is 80%, and the shape of the plastic zone changes from circular to oval with a major axis vertical. The plastic zone shape changes from oval to butterfly shape only when the stress exceeds the steady-state interval. Moreover, the stress sensitivity of the plastic zone is enhanced after assuming a butterfly shape. Meanwhile, a further dramatic and malignant expansion is produced.

### Numerical simulation study

To study the failure form and size characteristics of the surrounding rock in the mining-affected nearby goaf road in detail, FLAC<sup>3D</sup> numerical simulation software was used to conduct a numerical analysis combined with the histogram of the geological prospecting borehole and rock mechanics parameters, as shown in Table 1 for the mining-affected nearby goaf road of the 8202 fully mechanized face of the extra-thick coal seam. The length  $\times$  width  $\times$  height of the model was 400  $\times$  500  $\times$  150 m, as shown in Figure 8. The lateral and bottom surfaces of the model were fixed

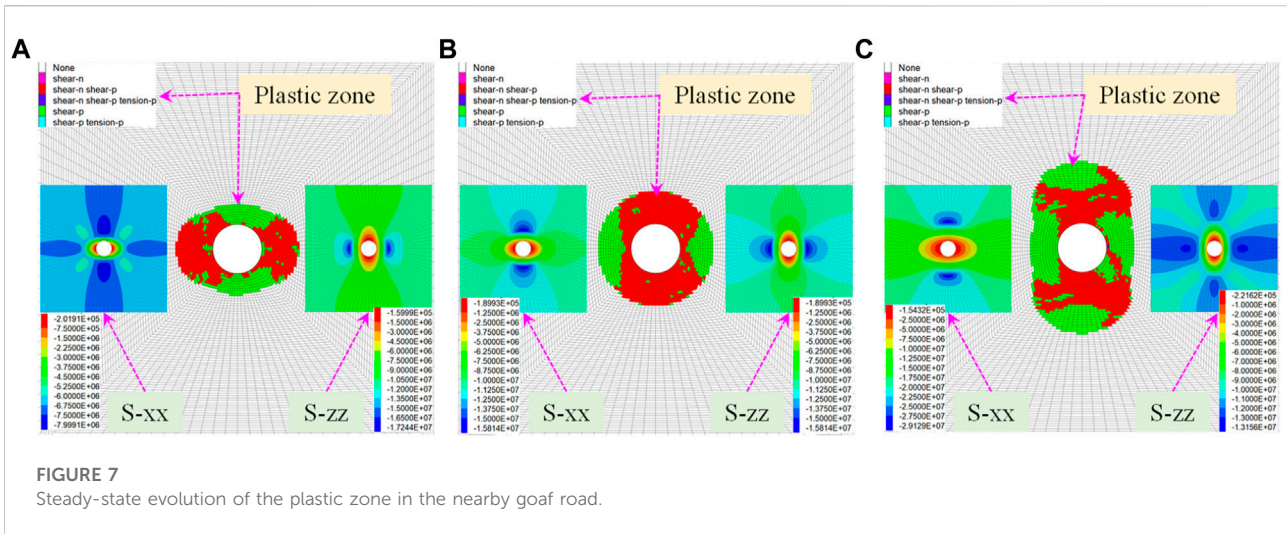


**FIGURE 7**  
Steady-state evolution of the plastic zone in the nearby goaf road.

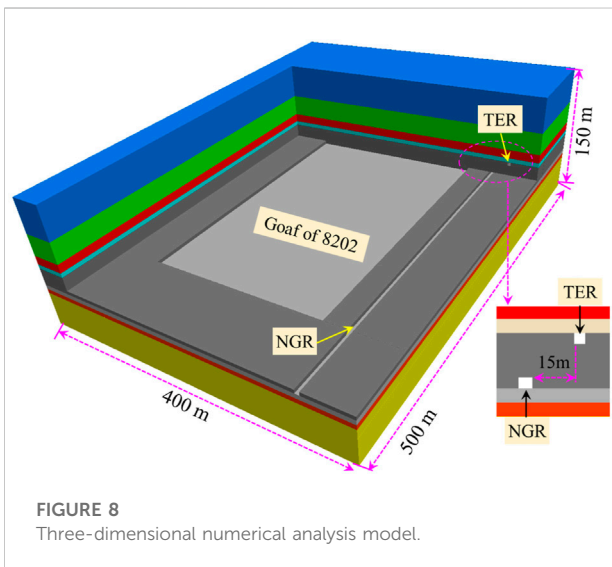


**FIGURE 8**  
Three-dimensional numerical analysis model.

constraints, and 9.5 MPa vertical stress was applied to the upper boundary (the buried depth of the top surface of model was 380 m). The Mohr–Coulomb criterion was employed, and the lateral pressure coefficient  $\lambda$  was 1.2. The width of the coal pillar in the nearby goaf road was 35 m. The road for the top excavation is driven along the roof of the coal seam. The nearby goaf road goes along the floor of the coal seam. The horizontal internal displacement of the two roads is 15 m, and the vertical distance is 18 m.

To accelerate the speed of the model calculation, the goaf of 8202 was filled by the double yield model, and its parameters are shown in Table 2.

When the 8202 working face is not mined, the stress and plastic zone range of the nearby goaf road are shown in Figure 9.

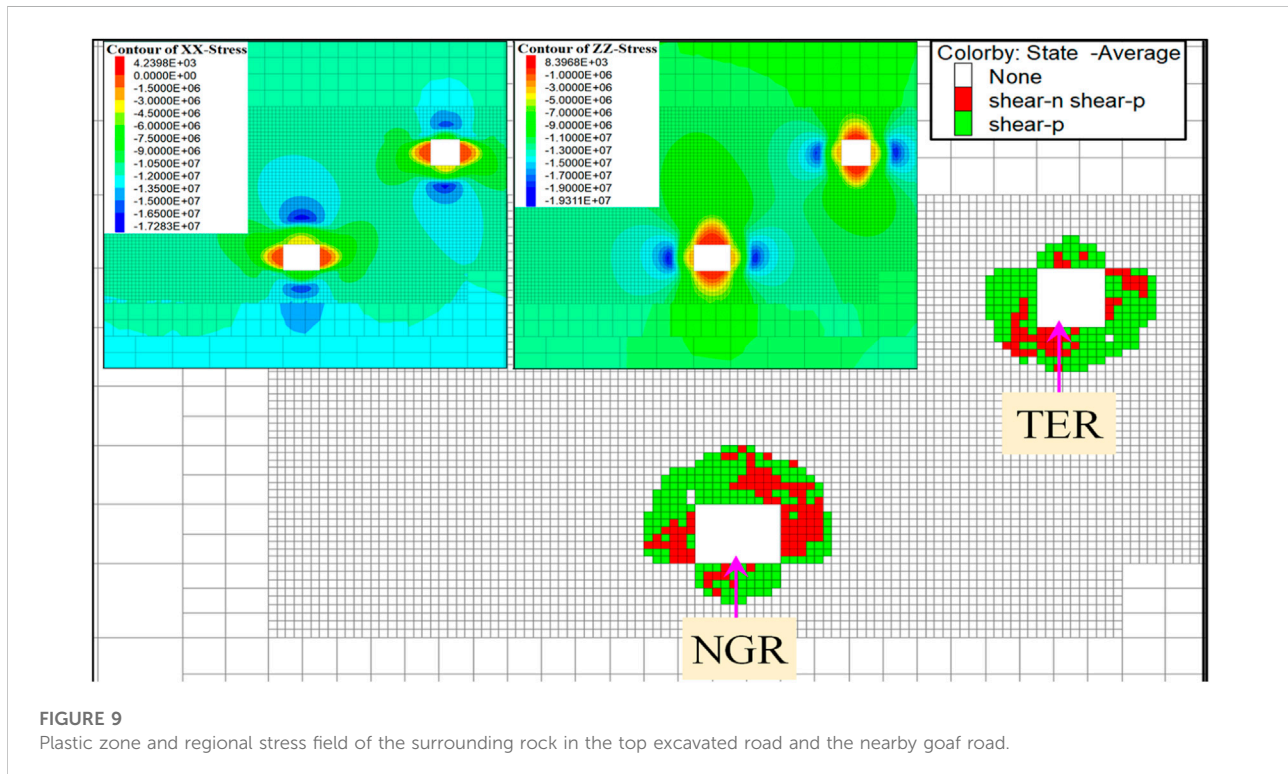
The symmetrical and uniform distribution of stress in the top excavating road leads to the symmetric development of the plastic zone in the surrounding rock. In the top excavating road, the plastic zone of the roof is 2 m and the plastic zone of the floor and side spans is 3 m. Because the coal seam lithology of the top excavating road is weak, the size of the plastic zone in the top excavating road is in the order: floor > sidewall > roof. Because the floor lithology of the nearby goaf road is larger than that of the coal seam, the shape and size of the plastic zone of the surrounding rock are opposite. The maximum dimensions of the plastic zone in the roof, sideboard, and floor are 4, 3, and 2 m, respectively. The plastic zone size of the nearby goaf road follows the order: roof > sidewall > floor. Due to the small vertical distance gap between the two roads, the maximum value of the stress concentration in the roads is basically the same, and the maximum value of the vertical stress and horizontal stress are 19.31 and 17.28 MPa, respectively. Furthermore, the horizontal spacing between the two roads is only 15 m, and the driving influence stress interaction concentration area is formed in the right side of the nearby goaf road and the left side of the top excavating road, which will affect the mining pressure appearance during the 8202 working face mining.

The plastic zone and regional stress field distribution of the surrounding rock are shown in Figure 10, when there is only a nearby goaf road. Although there is a 35 m protective coal pillar, the plastic zone of the goaf of the 8202 working face is related to the plastic zone of the nearby goaf road under the influence of lateral mining. The plastic zone of the surrounding rock of the nearby goaf road is considerably expanded, compared to that during tunneling. In addition to the rapid expansion of the side wall, the plastic zone of the front wall and the roof also likewise expanded from 3 to 4 m to 5.5 and 7 m, respectively. Corresponding to the plastic zone of the surrounding rock, the lateral horizontal stress of the goaf is in the recovery stage



TABLE 2 Mechanical parameters of the double yield model in goaf of the 8202 working face.

Bulk modulus/MPa (E)	Shear modulus/MPa (E)	Density/kg/m <sup>3</sup>	Dilation angle/°	Friction angle/°
6.833	5.653	1,650	8	26



(the maximum horizontal stress is only 25.00 MPa at the bottom boundary of the goaf) because of the pressure relief effect of the goaf. Meanwhile, the vertical direction amounts to a stress concentration (the maximum vertical stress is 34.82 MPa at 6 m of the front side, and the stress concentration coefficient is 1.79). The stress distribution also changes from symmetric to asymmetric. The lateral pressure coefficient at the vertical stress peak is 2.56. There is an asymmetric butterfly failure state in the nearby goaf road.

Compared with Figure 10, the plastic zone and vertical stress field of the surrounding rock of nearby goaf road both increase to a certain extent when there is a top excavating road. The maximum height of the plastic zone of the surrounding rock in the nearby goaf road roof reaches 8 m. The maximum vertical stress value increases from 34.82 to 35.73 MPa, as shown in Figure 11. There is a double vertical stress peak between the top excavating road and the nearby goaf road. The lateral pressure coefficient at the peak of vertical stress of the nearby goaf road likewise increases from 2.56 to 2.62. Due to the influence of the

bidirectional asymmetric mining stress, both the top excavating road and the nearby goaf road exhibit symmetrical failure. Meanwhile, the top excavating road further aggravates the degree of failure of the nearby goaf road.

## Mine pressure monitoring and analysis

### Monitoring scheme design

To master the change process of the surrounding rock and supporting body stress on the nearby goaf road, a bolt or cable dynamometer and borehole stress meter were used to monitor the change and evolution of the surrounding rock. Two groups of measuring stations were designed to be fitted with bolts and cable dynamometers. As shown in Figure 12, the distance between the two stations was 50 m. The first group of stations was 200 m in front of the nearby working



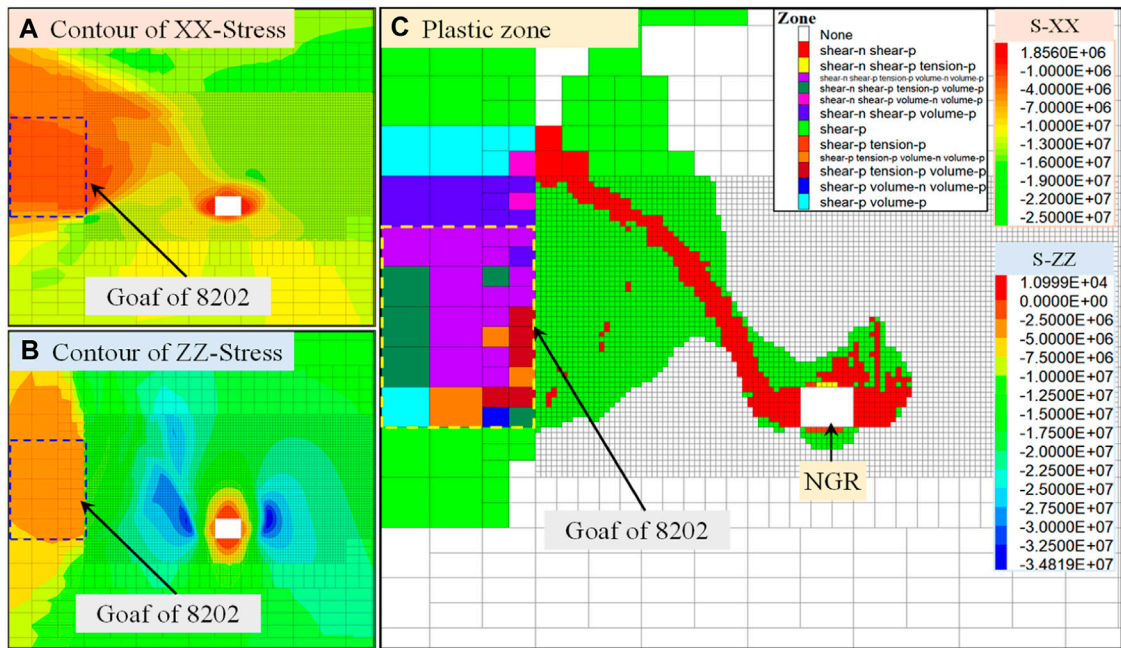


**FIGURE 10**  
Plastic zone and regional stress field distribution of the surrounding rock, only in the presence of the nearby goaf road.

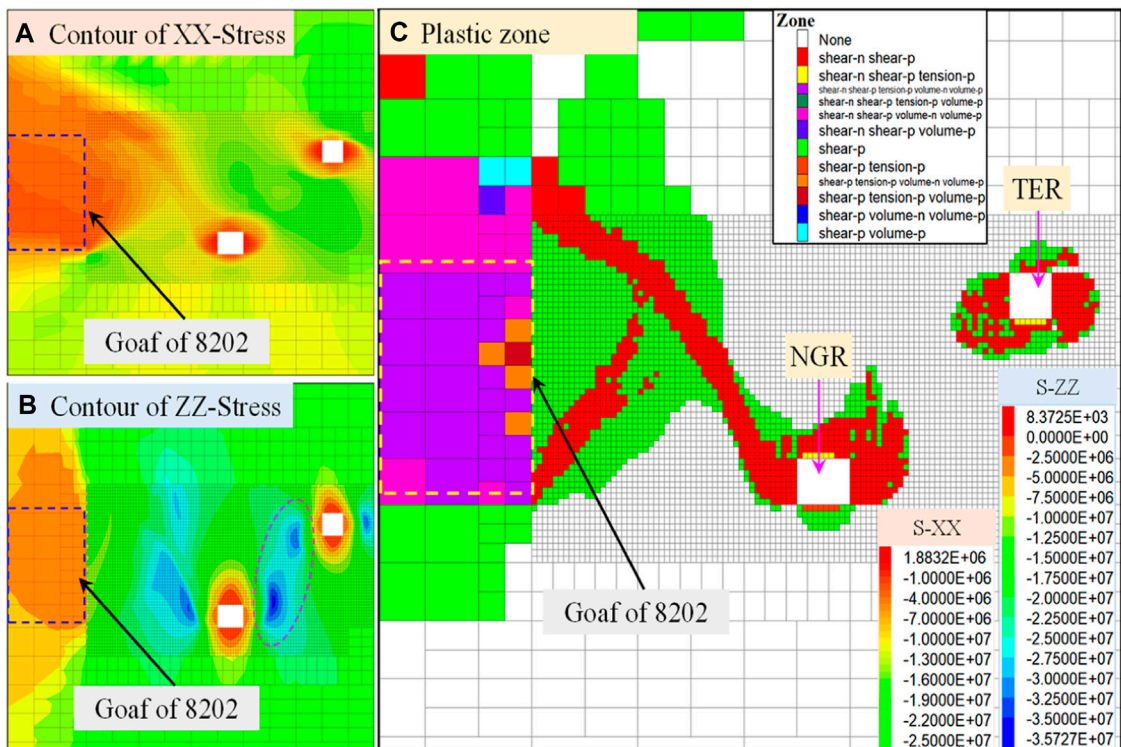
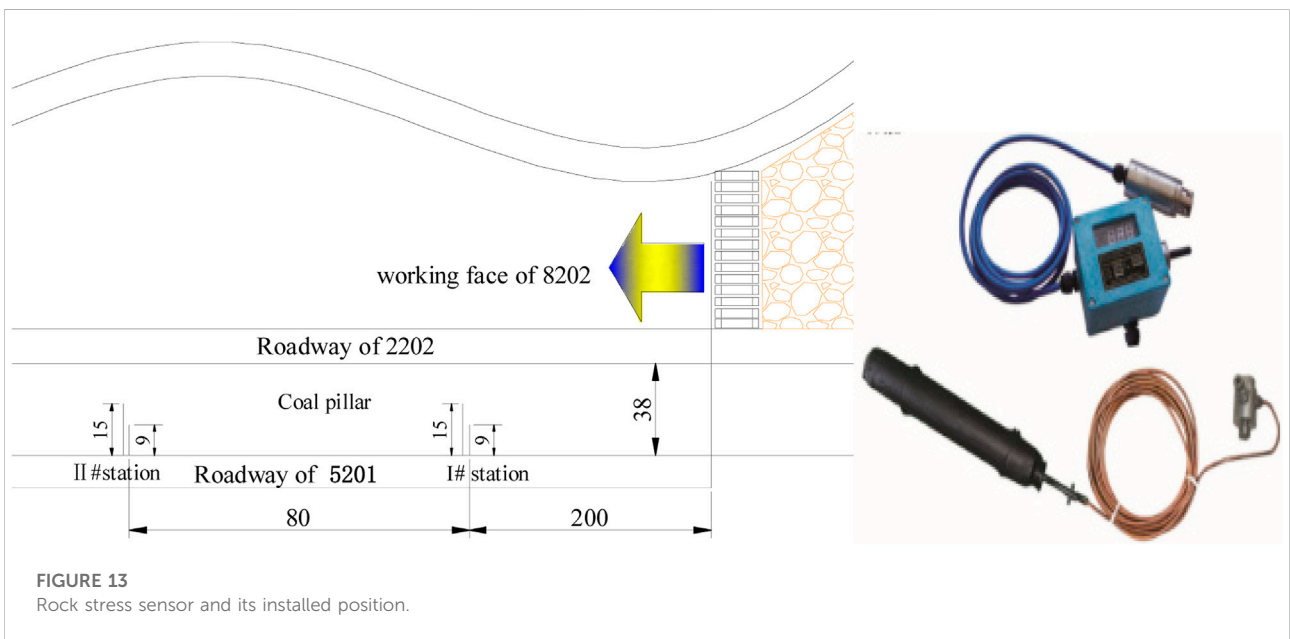
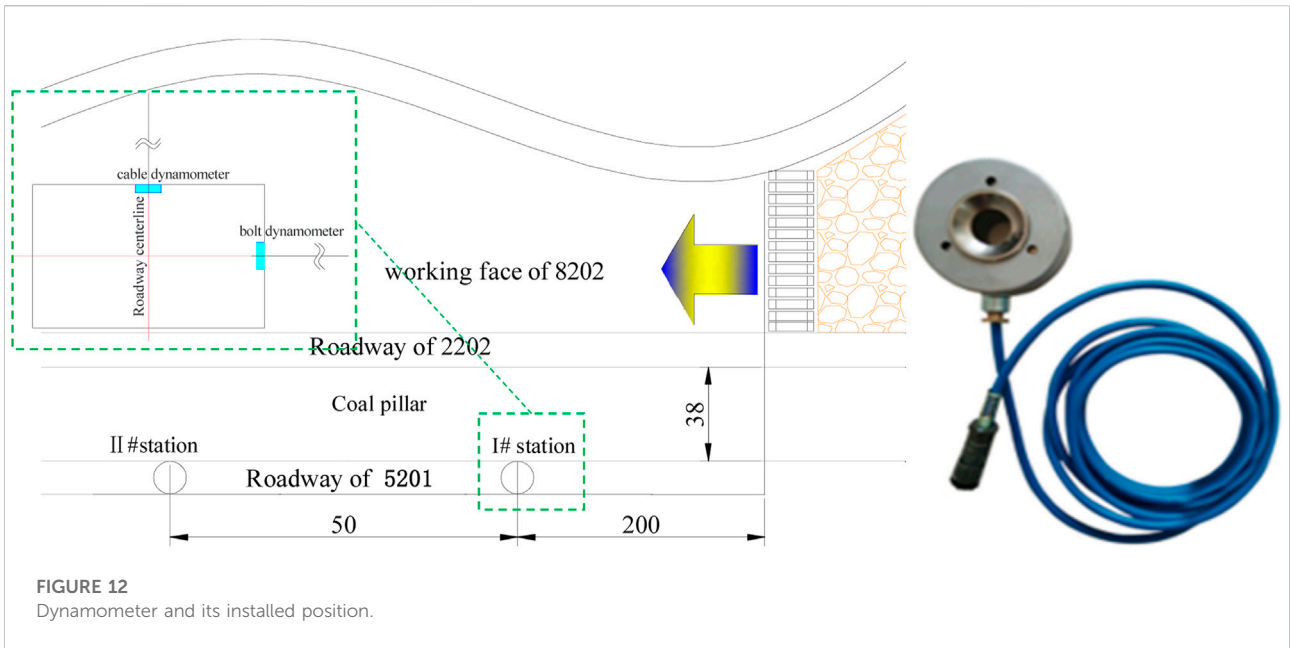


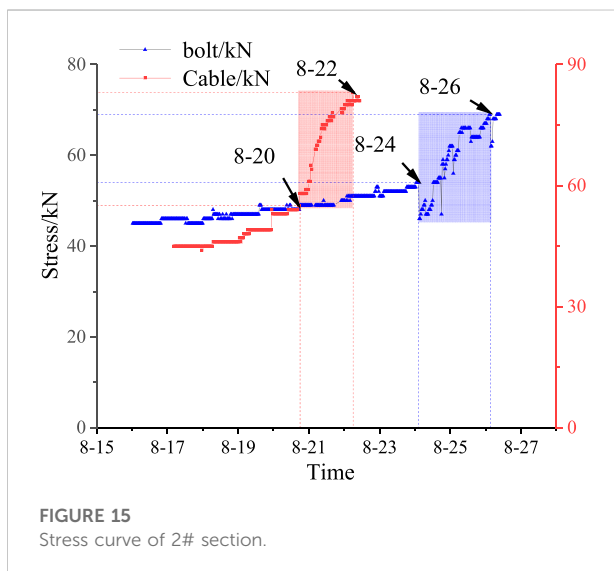
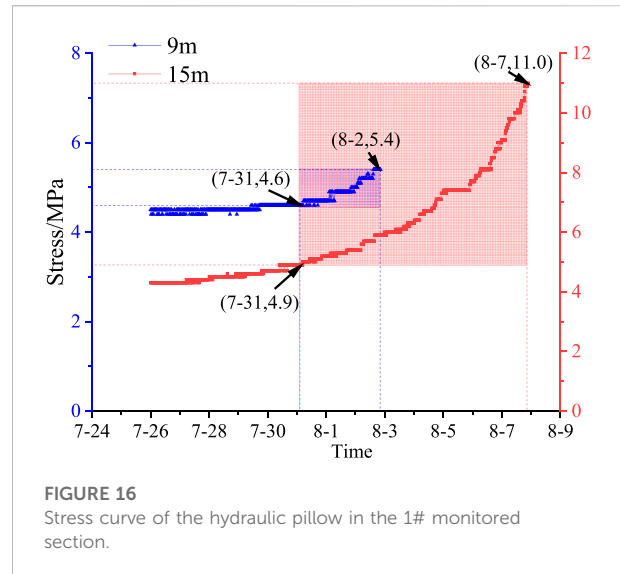
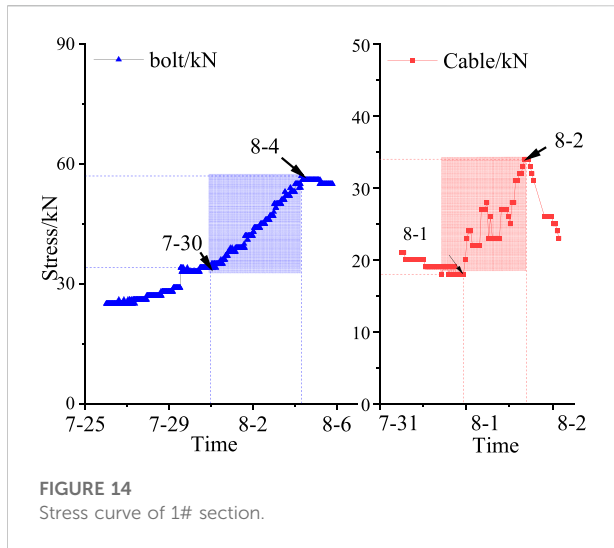
**FIGURE 11**  
Plastic zone and regional stress field distribution of the surrounding rock in TER and NGR.



face (the distance to open-off was 1,701.7 m). The cable dynamometer was settled in the roof and monitored the changes of roof pressure. At the same time, the bolt dynamometer was arranged at the side of the nearby goaf road and monitored the change of the road-side pressure.

The surrounding rock stress sensors were installed in the position as shown in Figure 13, and two test stations were set with

an interval of 80 m between each station. The first group of stations was 200 m away from the nearby working face (the distance to open-off was 1,703.7 m). Two hydraulic pillows were settled in each station. The depth of the hydraulic pillows was 9 and 15 m, respectively. The surrounding rock stress changes of the rock strata at different depths was monitored by each hydraulic pillow.



As shown in Figure 15, the bolt and cable stress began to change from August 20th and 24th, respectively, in the 2# monitoring section with the same trend. On August 20th, the cumulative stopping footage of the nearby working face was 1,714.2 m, and the distance of the horizontal position was 37.5 m from the equipment to the nearby working face. The peak of cable stress appeared on August 22nd (the distance was 30.8 m away from the equipment), and the stress peak of the bolt appeared on August 26th (the distance was 16.8 m away from the equipment).

This indicates that the influence of the lead abutment pressure on the surrounding rock of the nearby goaf road appeared about 30.2~37.5 m in front of the approaches to the working. The influence of the lead abutment pressure on the roof and two sides of the nearby goaf road in the carboniferous system was quite different. The peak stress on the side of the nearby goaf road appeared at 16.8~18.7 m from the nearby working face, and the peak value of stress on the roof appeared at 21.6~30.8 m. The lead abutment pressure caused the stress of the bolt, cable, and other supporting bodies to increase about 50%. The stress concentration coefficient of the supporting body in the roadway nearby goaf was about 1.5.

## Analysis of monitored data

### 1) Supporting body stress analysis of the bolt and cable

As shown in Figure 14, the bolt and cable stress respectively began to change from July 30th and August 1st in the 1# monitoring section. On July 30th, the cumulative stopping footage of the nearby working face was 1,671.5 m, and the distance of the horizontal position was 30.2 m from the equipment to the nearby working face. The peak cable stress appeared on August 2nd (the distance was 21.6 m away from the equipment), and the stress peak of the bolt appeared on August 4th (the distance was 18.7 m away from the equipment).

### 2) Monitoring data analysis of the surrounding rock stress sensor

As shown in Figure 16, the monitoring data of the 9 and 15 m hydraulic pillows began to increase from July 31st in the 1# monitoring section with the same increase trend. The data of the 9 m hydraulic pillow sensor grew more slowly than the 15 m. On July 31st, the cumulative stopping footage of the nearby working face was 1,671.5 m, and the horizontal distance was 32.2 m from the equipment to the nearby working face. The ratio of the peak

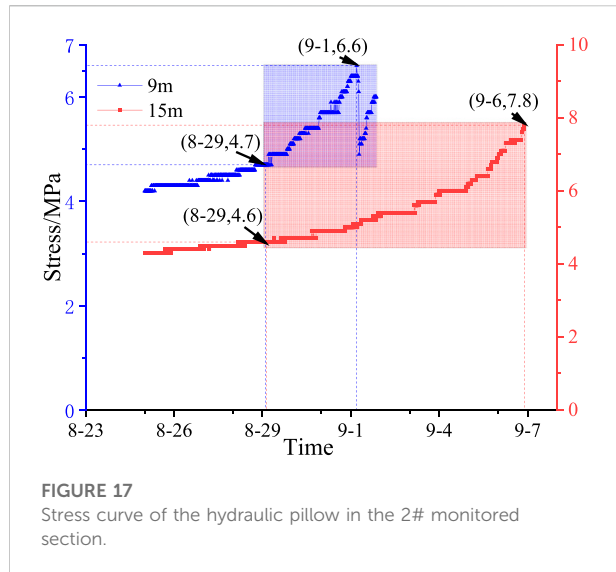


**FIGURE 17**  
Stress curve of the hydraulic pillow in the 2# monitored section.

point data to the initial change point data was used as the stress concentration factor. Therefore, the stress concentration coefficient of the surrounding rock at 9 m was 1.2, and at 15 m it was 2.2.

As shown in Figure 17, the monitoring data of the 9 and 15 m hydraulic pillows began to increase from August 29th in the 2# monitoring section with the same increase trend as the 1# monitoring section. On August 29th, the cumulative stopping footage of the nearby working face was 1,745.15 m, and the distance in the horizontal position was 38.6 m from the equipment to the nearby working face. The stress concentration coefficient of the surrounding rock at 9 m was 1.4, and at 15 m it was 1.7.

Therefore, the influence of the lead abutment pressure on the deep coal and rock of the coal pillar side begins to appear 32.2~38.6 m in front of the approaches to the working. The growth rate of deep stress was faster than that of shallow stress, and the stress increment in the shallow part was generally less than that in the deep part. The stress concentration coefficient at the depth of the coal pillar was approximately 1.7~2.2.

## Conclusion

Rock mechanics parameters were obtained by drilling cores and laboratory tests. Taking the Tong Xin coal mine as the research background, the law of strata pressure behavior of the surrounding rock in the nearby goaf road for the extra-thick coal seam in the Datong Mining area was analyzed, which provided

basic data for subsequent rock formation control. The following conclusions are obtained:

- 1) With the change of lateral pressure coefficient, the failure modes of the surrounding rock in the road assume the shapes of plastic zones that are circular, oval, and butterfly-shaped. When the plastic zone is circular or oval, the variation of the lateral pressure coefficient has little effect on the plastic zone. When the plastic zone of the surrounding rock presents the butterfly shape, a subtle change in the lateral pressure coefficient will cause a sharp expansion of plastic zone in the road of the extra coal seam.
- 2) Under the influence of mining, the asymmetric distribution of the regional stress field in the nearby goaf road of the extra coal seam leads to the butterfly failure of the surrounding rock. The auxiliary wall of the nearby goaf road is related to the 8202-goaf, which facilitates the induction of the surrounding rock instability. The existence of the top excavating road leads to the bimodal distribution of support pressure, which intensifies the failure range of the plastic zone in the nearby goaf road, such that the instability probability of the surrounding rock increases.
- 3) The influence of the lead abutment pressure on the surrounding rock of the nearby goaf road begins to appear about 30 m in front of the extra coal-seam working face. The influence of the lead abutment pressure on the roof and two sides of roadway is quite different. The deep coal and rock stress level and growth rate are faster than the shallow ones of the surrounding rock in the road. The stress concentration coefficient at the pillar side is about 1.8~2.2, and its deviatoric stress level is higher. This increases the instability and risk of damage of the nearby goaf road.

## Data availability statement

The original contributions presented in the study are included in the article/Supplementary Material, and further inquiries can be directed to the corresponding author.

## Author contributions

XL: conceptualization, methodology, and writing—original draft. CL: formal analysis and data curation. JL: visualization and software. LW: project administration.

## Funding

This study was supported by the National Natural Science Foundation of China (52004289).



## Conflict of interest

XL and LW were employed by the company Uroica (Shandong) Mining Technology Co., Ltd. and CL was employed by the company CCTEG Wuhan Engineering Company.

The remaining author declares that the research was conducted in the absence of any commercial or financial relationships that could be construed as a potential conflict of interest.

## References

- Chaojiong, H., Xiangyu, W., Jianbiao, B., Ningkan, M., and Wendan, W. (2021). Basic theory and technology study of stability control for surrounding rock in deep roadway. *J. China Univ. Min. Technol.* 50, 1–12. doi:10.13247/j.cnki.jcmt.001242
- Chen, L., Wenlong, Z., Ning, W., and Cheng, H. (2019). Roof stability control based on plastic zone evolution during mining. *J. Min. Saf. Eng.* 36, 753–761. doi:10.13545/j.cnki.jmse.2019.04.014
- Deng-hong, C., Xin-zhu, H., Ya-wei, D., and Shi-xing, C. (2016). Simulation of zonal tensile and compressive deformation and failure of surrounding rock in deep large deformation mining gateway. *Rock Soil Mech.* 37, 2654–2662. doi:10.16285/j.rsm.2016.09.030
- Detournay, E., and John, C. M. S. (1988). *Design charts for a deep circular tunnel under non-uniform loading Rock Mechanics and Rock Engineering 21*. Rock Mechanics and Rock Engineering.
- Ding, S., Gao, Y., Jing, H., Shi, X., Qi, Y., and Guo, J. (2021). Influence of weak interlayer on the mechanical performance of the bolted rock mass with a single free surface in deep mining. *Miner. (Basel)*, 11, 496. doi:10.3390/min11050496
- Du, H., Song, D. Q., Chen, Z., and Guo, Z. Z. (2020). Experimental study of the influence of structural planes on the mechanical properties of sandstone specimens under cyclic dynamic disturbance. *Energy Sci. Eng.* 8, 4043–4063. doi:10.1002/ese3.794
- Du, H., and Song, D. Q. (2022). Investigation of failure prediction of open-pit coal mine landslides containing complex geological structures using the inverse velocity method. *Nat. Hazards (Dordr)*, 111, 2819–2854. doi:10.1007/s11069-021-05159-w
- Guo, X., Guo, L., and Jiang, B. (2020). *Elliptic equation of plastic area boundary around the circular laneway in nonuniform stress field shock and vibration 2020*. Shock and Vibration, 1–9. doi:10.1155/2020/8849579
- Guo, X., Zhao, Z., Gao, X., Wu, X., and Ma, N. (2019). Analytical solutions for characteristic radii of circular roadway surrounding rock plastic zone and their application. *Int. J. Min. Sci. Technol.* 29, 263–272. doi:10.1016/j.ijmst.2018.10.002
- Guo, X. F., Li, C., and Huo, T. H. (2021). Shapes and formation mechanism of the plastic zone surrounding circular roadway under partial confining stress in deep mining. *Geomechanics Eng.* 25, 509–520. doi:10.12989/gae.2021.25.6.509
- Hongpu, K., et al. (2019). Forty years development and prospects of underground coal mining and strata control technologies in China. *J. Min. Strata Control Eng.* 1, 7–39. doi:10.13532/j.jmsce.cn10-1638/td.2019.02.002
- Hongpu, K. (2020). Temporal scale analysis on coal mining and strata control technologies. *J. Min. Strata Control Eng.* 2, 5–30. doi:10.13532/j.jmsce.cn10-1638/td.20200119.001
- Hongtao, L., Xiangye, W., Zhen, H., Xidong, Z., and Xiaofei, G. (2017). Evolution law and stability control of plastic zones of retained entry of working face with double roadways layout. *J. Min. Saf. Eng.* 34, 689–697. doi:10.13545/j.cnki.jmse.2017.04.013
- Housheng, J., Nianjie, M., and Qiankun, Z. (2016). Mechanism and control method of roof fall resulting from butterfly plastic zone penetration. *J. China Coal Soc.* 41, 1384–1392. doi:10.13225/j.cnki.jccs.2015.1367
- Jia, H. S., Pan, K., Liu, S. W., Peng, B., and Fan, K. (2019). Evaluation of the mechanical instability of mining roadway overburden: Research and applications. *Energies (Basel)*, 12, 4265. doi:10.3390/en12224265
- Jian-biao, B. L., Xiang-yu, W., and Zhe, Y. (2007). Study of coupling support in soft rock roadway under high stress. *J. China Univ. Min. Technol.*, 421–425. doi:10.3321/j.issn:1000-1964.2007.04.001
- Kaizong, X., Congxin, C., Tianlong, W., Yun, Z., and Yue, W. (2022). Estimating the geological strength index and disturbance factor in the Hoek–Brown criterion using the acoustic wave velocity in the rock mass. *Eng. Geol.* 306, 106745. doi:10.1016/j.enggeo.2022.106745
- Li, C., Guo, X. F., Lian, X. Y., and Ma, N. J. (2020a). Failure analysis of a pre-excavation double equipment withdrawal channel and its control techniques. *Energies* 13, 6368. doi:10.3390/en13236368
- Li, C., Wu, Z., Zhang, W. L., Sun, Y. H., Zhu, C., and Zhang, X. H. (2020b). A case study on asymmetric deformation mechanism of the reserved roadway under mining influences and its control techniques. *Geomechanics Eng.* 22, 449–460. doi:10.12989/gae.2020.22.5.449
- Li, Q. H., Song, D. Q., Yuan, C. M., and Nie, W. (2022). An image recognition method for the deformation area of open-pit rock slopes under variable rainfall. *J. Meas.* 188, 110544. doi:10.1016/j.measurement.2021.110544
- Pu, W., Baisheng, Z., Lei, W., Xueyao, L., Xiaofei, S., and Junqing, G. (2020). Research on roof falling mechanism and support technology of mining roadway in expansive soft rock. *J. Min. Strata Control Eng.* 2, 57–65. doi:10.13532/j.jmsce.cn10-1638/td.20191220.001
- Qihang, L., Jiabo, G., Danqing, S., Wen, N., Pooya, S., and Jiangtong, L. (2022). Automatic recognition of erosion area on the slope of tailings dam using region growing segmentation algorithm. *Arab. J. Geosci.* 15, 438. doi:10.1007/s12517-022-09746-4
- Qingfeng, H., Ximin, C., Wenkai, L., Tangjing, M., and Haoran, G. (2020). Law of overburden and surface movement and deformation due to mining super thick coal seam. *J. Min. Strata Control Eng.* 2, 31–39. doi:10.13532/j.jmsce.cn10-1638/td.20191113.001
- Tian, Z., and Yiliang, W. (2020). Study on deformation evolution law and support technology of surrounding rock in multiple mining roadway. *J. Min. Strata Control Eng.* 2, 66–73. doi:10.13532/j.jmsce.cn10-1638/td.20200106.001
- Xia, K., Chen, C., Wang, T., Yang, K., and Zhang, C. (2022). *Investigation of mining-induced fault reactivation associated with sublevel caving in metal mines*. Engineering Geology doi:10.1007/s00603-022-02959-9
- Xiaofei, G. (2019). *Criterion of plastic zone shapes of roadway surrounding rock and its application*. Beijing: China University of Mining and Technology (Beijing) Doctoral dissertations.
- Xie, G., Chuanming, L., and Lei, W. (2016). Mechanical characteristics and practical application on stress shell of roadway surrounding rock. *J. China Coal Soc.* 41, 2986–2992. doi:10.13225/j.cnki.jccs.2016.0238
- Xie, G., Hao, F., and Lei, W. (2019). Evolution law and engineering application of surrounding rock force chain in shallow coal seam working face. *J. China Coal Soc.* 44, 2945–2952. doi:10.13225/j.cnki.jccs.2019.0706
- Yongen, L., Xiaofei, G., Nianjie, M., Chen, L., and Tianhong, H. (2021). Research status and evaluation of theoretical calculation of plastic zone boundary for hole surrounding rock. *Coal. Sci. Technol.* 49, 141–150. doi:10.13199/j.cnki.cst.2021.05.018
- Zhang, L., Huang, M., Xue, J., Li, M., and Li, J. (2021). Repetitive mining stress and pore pressure effects on permeability and pore pressure sensitivity of bituminous coal. *Nat. Resour. Res.* 30, 4457–4476. doi:10.1007/s11053-021-09902-9
- Zhao, Z., Nianjie, M., Hongtao, L., and Xiaofei, G. (2018). A butterfly failure theory of rock mass around roadway and its application prospect. *J. China Univ. Min. Technol.* 47, 969–978. doi:10.13247/j.cnki.jcmt.000922
- Zhen, G. (2018). *Evolution law of plastic zone and burst failure mechanism of gateway in yima coalfield*. Beijing: China University of Mining and Technology (Beijing) Doctoral dissertations.
- Zhiqiang, Z. (2014). *Mechanism of surrounding rock deformation and failure and control method research in large deformation mining roadway*. Beijing: China University of Mining and Technology (Beijing) Doctoral dissertations.

## Publisher's note

All claims expressed in this article are solely those of the authors and do not necessarily represent those of their affiliated organizations, or those of the publisher, the editors, and the reviewers. Any product that may be evaluated in this article, or claim that may be made by its manufacturer, is not guaranteed or endorsed by the publisher.